NORMAL FINGER PROXIMAL INTERPHALANGEAL (P. I. P. -) JOINT SURFACES SHOW ASYMMETRIES AND INCONGRUENCES IN THE CORONAL (FRONTAL) PLANE

K. J. van Zwieten [1], P. Adriaensens [1], L. Kosten [1], S. De Munter [1], K. P. Schmidt [1], S. A. Varzin [2, 3], O. E. Piskun [3]*

[1] Department of Anatomy, Functional Morphology, BioMed Research Institute, Faculty of Medicine and Life Sciences, University of Hasselt, Diepenbeek, Belgium,
[2] Department of Intermediate Level Surgery, Faculty of Medicine, St. Petersburg State University, St. Petersburg, Russia,
[3] Department of Physical Culture and Adaptation, Peter-the-Great St. Petersburg Polytechnic University, St. Petersburg, Russia.

* koosjaap.vanzwieten@uhasselt.be

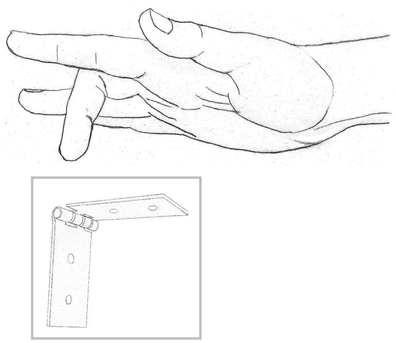

Figure 1. The P.I.P.-joint of the finger (top) is for convenience classified as a hinge joint (bottom).

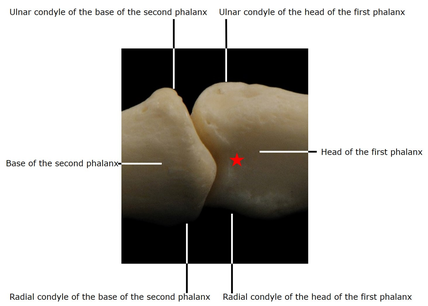

Figure 2. Osteology P.I.P.-joint, right index finger, dorsal view, ★ indicates intercondylar groove at head of first phalanx.

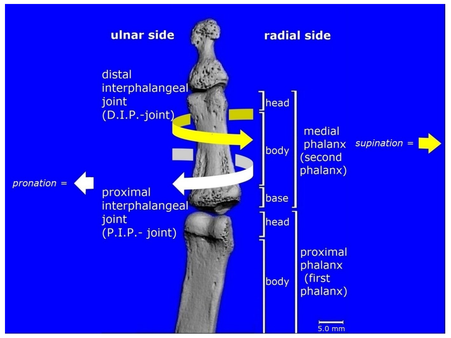

Figure 3. More osteology and terms of rotation, in the right index finger, palmar view.

Technical data HR-MRI

Varian 400 spectrometer, 9,4 T superconducting magnet. Field of view FOV (mm) in frontal plane: 25 x 25; imaging data matrix of 704 x 350; pixel resolution (µm) 71 x 71,5. Further acquisition parameters: repetition time TR: 2500 ms; echo time TE: 18 ms; number of averages NA = 24; slice thickness 2 mm.

An otherwise normal anatomical specimen of an extended right third finger was used. In Fig. 4, the "blue plane" represents the level of slicing; ↔ indicates the resulting frame length.

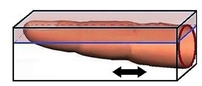

Figure 4. The blue plane (frontal = coronal) indicates the level of HR-MRI slicing.

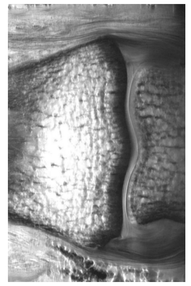

Figure 5. The resulting HR-MRI slice in the frontal (coronal) plane.

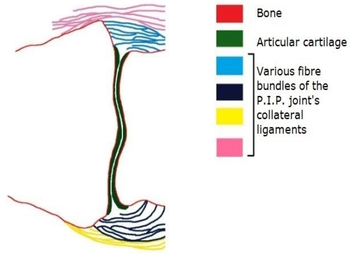

Figure 6. Main structures of Fig. 5, indicated by colour code.

INTRODUCTION

Movement possibilities of normal proximal interphalangeal (P.I.P.-) joints in human fingers were recently analysed, anatomically (1). As also seen *in vivo* at our own fingers (Fig. 1, top) (2), the P.I.P.- joint is for convenience classified as a *hinge joint* (Fig. 1, bottom) (3). Careful observation, however, reveals extra movement possibilities, namely (modest) longitudinal rotations of the P.I.P.- joint (Fig. 3) (4, 5). By plane geometry applied in frontal (coronal) plane HR-MRI of the mating articular surfaces *in situ,* we elucidated their asymmetries and incongruences. To our knowledge, these have only been analysed earlier by *osteology* (6).

OBJECTIVES

Our outcome data may help to design better close-to-reality P.I.P - arthroplasties (artificial joints), in order to relieve *osteoarthritis (OA)* and *rheumatoid arthritis (RA)* (7).

RESEARCH QUESTIONS, MATERIAL AND METHODS

As (4) rightly states, "the asymmetry of the condylar surfaces in the anteroposterior plane would require a profile projector to be analysed more accurately". Therefore, by using such profiles in the frontal (= coronal) plane, as presented in the HR-MRI frame (Fig. 5), we first wished to quantify the asymmetries of the radial and the ulnar condyles (Fig. 2). This was done by superimposing a grid (8) on the frame (Fig.7). Second, by analysing the contours in frontal plane of the *mating* condyles (concave at base of second phalanx, and convex at head of first phalanx), we examined to what extent these articular curvatures match. Therefore we constructed their radii in plane geometry (9) (Fig. 8) with computer graphics (10). Shorter radii mean stronger convexities / concavities (and *v.v.*)

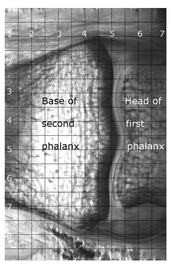

Figure 7. Superimposed grid reveals asymmetries of the condyles (see also Figs. 2, 3 & 5).

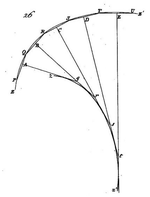

Figure 8. Geometric method to construct the radii of a given curve by the perpendicular bisectors of the inscribed open polygon formed by its successive chords [*after* (9)]. From their points of intersection, shorter radii correspond with a more convex curvature.

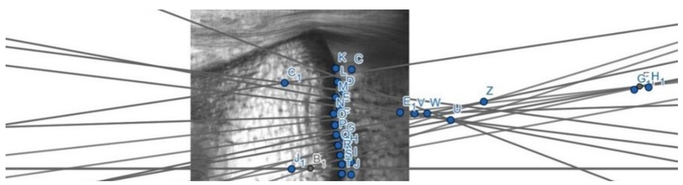

Figure 9 a. HR-MRI-slice of Fig. 5, *ulnar* condyles with their inscribed polygons, perpendicular bisectors, and points of intersection. Further: see text.

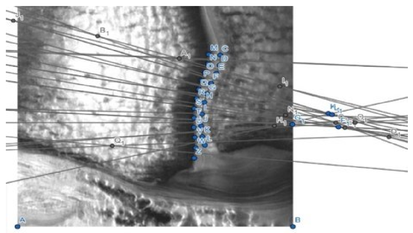

Figure 9 b. As in Fig. 9 a - but here with respect to the pair of *radial* condyles.

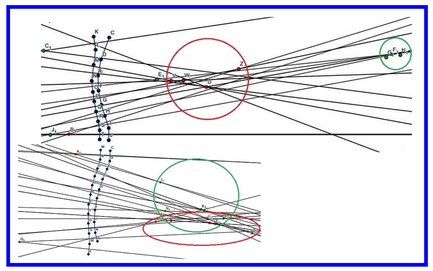

Figure 10. Both geometric constructions combined in one frame.

RESULTS (1)

As already suggested by Figs. 2 and 3 of the proximal interphalangeal (P.I.P. -) joint, its ulnar condyles are somewhat bigger than the radial condyles, at the base of the second phalanx as well as at the head of the first phalanx. This is the case in the index finger and in the third finger. In the fourth and in the fifth finger however, the radial condyles are bigger (1). Superimposing a grid on the HR-MRI frontal (= coronal) slice of Fig. 5 reveals that the curvature of the ulnar condyle at the base of the second phalanx amounts about 5 squares, the curvature of the radial condyle about 4 squares. The same applies to the mating articular curvatures at the head of the first phalanx.

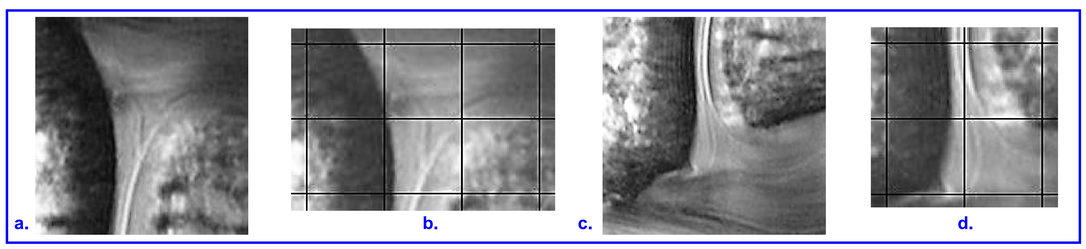

Figure 11 a - d. Quantifying the sizes of the ulnar (a, b) and the radial (c, d) *plicae synoviales* (details of Fig. 5). For further explanation, see right text block →

RESULTS (2)

The two pairs of curvatures of the articular surfaces were analysed separately. In Fig. 9 a, the chords of the ***ulnar*** curvatures are plotted on the HR-MRI-slice, resulting in the inscribed open polygon C-J for the curvature of the articular surface of the first phalanx. A comparable graphical construction gave the inscribed open polygon K-T for the second phalanx. With mathematical computer graphics (10), we constructed the perpendicular bisectors of the chords of both curvatures. This resulted in points of intersection of these bisectors, respectively U, V, W, Z, and B_1 for the ulnar articular surface of the first phalanx, and C_1, E_1, F_1, H_1, and J_1 for the ulnar articular surface of the second phalanx. Fig. 9 b shows a similar procedure, applied to curvatures on HR-MRI-slice of the ***radial*** condyles and their corresponding polygons and points of intersection.

Fig. 10 shows both graphical constructions combined in one frame, at the same scale. Set of intersection points of first phalanx circled in red, of second phalanx in green. For the radial articular curvatures, red and green areas partly overlap. For the ulnar curvatures, red and green areas are separate, green areas corresponding with longer radii It means, that the convexity of the proximal radial condyle here corresponds with its mating concavity of the distal radial condyle, so: at the ***radial*** side they are fairly congruent. At ***ulnar*** side however, the articular curvature of the proximal condyle shows stronger convexity, compared with its mating concavity of the distal condyle. They are incongruent.

ADDITIONAL MEASUREMENTS

Within the P.I.P.-joint, the outer edges of the condyles are accompanied by wedge-shaped soft tissues consisting of the thin synovial lining at the inner side of the joint capsule. They small structures contribute to the close-packed position of all elements normally constituting a synovial joint. These so-called *plicae synoviales* (or synovial folds) are recognised in our HR-MRI by their triangular appearance (Figs. 5 & 11). They thus show a somewhat V-like and Λ-like form, in the frontal HR-MRI slice, respectively at the ulnar and the radial side (Figs. 11 a & c). By the superimposed grid (8) their sizes were also quantified, namely about 1 vs. 1,5 squares respectively (Figs. 11 b & d). This means, that here the larger (ulnar) condyles have a smaller synovial fold, whereas the smaller (radial) condyles are accompanied by a larger synovial fold.

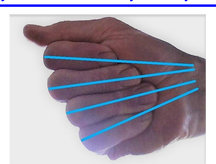

Fig. 12. In P.I.P.-flexion, fingers converge towards one point.

SUMMARY, AND SOME FUNCTIONAL ASPECTS

In the 3rd finger's P.I.P. - joint, asymmetries of its condyles imply that ulnar condyles are ± ¼ larger than radial ones. The articular surface of the **ulnar** condyle of the first phalanx is more convex, compared to its mating articular surface of the second phalanx. Ulnar condyles show an incongruence of the articular surfaces: greater convexity of the "ball", and a lesser concavity of its "socket", thus allowing (small) additional translations to occur. The convex articular surface of the **radial** condyle of the first phalanx nicely fits in with its mating concave articular surface of the radial condyle of the second phalanx. So, radial articular surfaces of both condyles of the P. I. P.- joint are fairly congruent, approaching a ball-and-socket-like situation. P.I.P. axial rotational motions thus can occur. Each individual P.I.P.- joint of fingers 2 - 5 exhibits its own corresponding range of such a *pronation* and *supination* (Fig. 3) (5). In the living this can be demonstrated, especially at full P.I.P. - flexion in which these rotations together result in directions of all fingers 2-5 converging towards *one point* (Fig. 12) (12).

REFERENCES

1. Van Zwieten K. J., Schmidt K. P., Adriaensens P., De Munter S., Kosten L., Piskun O. E., Varzin S. A. (2020) Asymmetries and incongruences of articular surfaces of P.I.P.- joint in normal human finger, in: Health the base of Human Potential: Problems and ways to solve them, ISSN 2076-4618, 720-732. *Figures used by permission*
2. Landsmeer J. M. F. (1976) Atlas of Anatomy of the Hand. Edinburgh, London, New York: Churchill Livingstone. *Artist's impression,* inspired by its Fig. 9.6 b, on p. 319.
3. Abaci T., Mortara M., Patane G., Spagnulo M., Vexo F., Thalmann D., Bridging Geometry and Semantics for Object Manipulation and Grasping (2005) Proceedings of Workshop towards Semantic Virtual Environments' (SVE 2005). University of Geneva, Villars, Switzerland, 110-119.
4. Dubousset J. F. (1980) Les phénomènes de rotation axiale lors de la prise au niveau des doigts. (The phenomena of axial rotation when gripping at the level of the fingers). In: Tubiana, R. (Ed.) Traité de chirurgie de la main, Vol. I, Paris, Masson, 238-242.
5. Degeorges R., Laporte S., Pessis E., Mitton D., Goubier J. N., Lavaste, F. (2004) Rotations of three joint fingers: a radiological study. Surgical and Radiologic Anatomy, 26, 392-398.
6. Dumont C., Albus G., Kubein-Meesenburg D., Fanghänel J., Stürmer K. M., Nägerl H. (2008) Morphology of the interphalangeal joint surface and its functional relevance. Journal of Hand Surgery, 33A, 9-18.
7. Schindele S. (2019) Gelenkersatz am Fingermittelgelenk (Arthroplasty at the proximal interphalangeal joint). Orthopäde, 48, 5, 378-385.
8. http://www.timgagnon.com/grid/ Accessed on January 30, 2021.
9. Schmidt I. R. (1837) Beginselen der Differentiaal en Integraal Rekening (The Principles of the Differential and Integral Calculus), 2nd Edition. 's-Gravenhage, Amsterdam, The Netherlands, Uitgeverij De Gebroeders Van Cleef, p. 211; Pl. III, Fig. 26.
10. https://www.geogebra.org/geometry/ Accessed on January 30, 2021.
11. Koo S., Andriacchi T. P. (2008) The knee joint center of rotation is predominantly on the lateral side during normal walking. Journal of Biomechanics, 41, 6, 1269-1273.
12. Kapandji I. A. (2007) The Physiology of the Joints, Volume 1, The Upper Limb, 6th Edition, Edinburgh etc., Churchill Livingstone, 206-207.